Received January 1996
Revised November 1996

Transient free convection past a semi-infinite vertical plate with variable surface temperature

H.S. Takhar
Department of Engineering, Manchester University, Manchester, UK
P. Ganesan
Department of Mathematics, College of Engineering, Anna University, Madras, India
K. Ekambavanan
School of Architecture and Planning, Anna University, Madras, India, and
V.M. Soundalgekar
Brindavan Society, Thane, India

Introduction

Natural convection heat transfer plays an important role in our environment and in many engineering devices. The buoyancy force induced by density differences in a fluid causes natural convection. The study of natural convection flow past a semi-infinite plate was first made by Pohlhausen[1] using an integral method, whereas the similarity method was first used to study this problem by Ostrach[2] and the resulting non-linear ordinary differential equations were solved computationally. Later on many papers were published on this topic assuming different types of physical conditions, and these theoretical predictions were confirmed by means of experiments. The more difficult problem of transient free convection flow past a semi-infinite vertical isothermal plate was first studied by Siegel[3] using an integral method. Both isothermal and constant heat flux conditions were considered in this paper. Later, Hellums and Churchill[4] were the first to study this problem for a semi-infinite vertical plate by using an explicit finite-difference technique which is conditionally stable and convergent. Soundalgekar and Ganesan[5] have studied transient free convection flow by using an implicit finite-difference technique, and by employing the Crank-Nicolson type of difference scheme which is unconditionally stable and convergent. Ede[6] reviewed this transient heat transfer on vertical surfaces under different wall conditions. However, when the surface heating is non-uniform, the steady-state free convection problem for a semi-infinite vertical plate becomes quite complicated. This was

International Journal for Numerical Methods for Heat & Fluid Flow
Vol. 7 No. 4, 1997, pp. 280-296.

studied by Sparrow and Gregg[7] by assuming the power-law variation of the wall temperature $T_w'(x) - T'_\infty = ax^n$, where a is a constant. Another review of transient natural convection was presented by Raithby and Hollands[8], wherein a large number of papers on this topic were referred. In this review, the meaning of transient convection has been explained systematically. They have defined the conduction regime and the steady-state regime and that which lies between these two regimes as the transient regime. The behaviour of fluid motion during this transient regime is useful in understanding the physical situation in many engineering applications. The transient free convection flow past a semi-infinite vertical plate with power-law variation of the temperature has not received the attention of researchers and hence it is now proposed to study this important physical phenomenon. In the next section, the mathematical analysis is presented, followed by the results and discussions and, finally, the conclusions are set out.

Mathematical analysis

We consider here the unsteady flow of a viscous incompressible fluid past a semi-infinite vertical plate. The x-axis is taken along the plate in the vertically upward direction and the y-axis is chosen perpendicular to the plate at the leading edge. The gravitational acceleration, g, is acting downward. Initially, it is assumed that the plate and the fluid are at the same temperature T'_∞. At time $t' \geq 0$, the plate temperature is assumed to vary as $T' = T'_w(x) - T'_\infty = ax^n$. It is also assumed that the fluid properties are constant except for the density variation that induces the buoyancy force. By assuming the Boussinesq approximation, the unsteady two-dimensional boundary layer flow can be shown to be governed by the following equations:

$$\frac{\partial u}{\partial x} + \frac{\partial v}{\partial y} = 0 \tag{1}$$

$$\frac{\partial u}{\partial t'} + u\frac{\partial u}{\partial x} + v\frac{\partial u}{\partial y} = g\beta(T' - T'_\infty) + \nu\frac{\partial^2 u}{\partial y^2} \tag{2}$$

$$\frac{\partial T'}{\partial t'} + u\frac{\partial T'}{\partial x} + v\frac{\partial T'}{\partial y} = \alpha\frac{\partial^2 T'}{\partial y^2} \tag{3}$$

Here u and v are the velocity components in the x and y directions respectively, t' the time, ν the kinematic viscosity, β the coefficient of volume expansion, T' the temperature of the fluid in the boundary layer, T'_∞ the temperature of the fluid far away from the plate and α is the thermal diffusivity.

The initial and boundary conditions are given by:

$$\left.\begin{array}{lll} t' \le 0,\ u = 0,\ v = 0,\ T' = T'_\infty & & \\ t' > 0,\ u = 0,\ v = 0,\ T' = T'_\infty + ax^n & \text{at } y = 0 & \\ u = 0,\ T' \to T'_\infty & \text{at } x = 0 & \\ u \to 0,\ T' \to T'_\infty & \text{as } y \to \infty & \end{array}\right\} \quad (4)$$

Equations (1)-(4) reduce to the following non-dimensional form:

$$\frac{\partial U}{\partial X} + \frac{\partial V}{\partial Y} = 0 \quad (5)$$

$$\frac{\partial U}{\partial t} + U\frac{\partial U}{\partial X} + V\frac{\partial U}{\partial Y} = T + \frac{\partial^2 U}{\partial Y^2} \quad (6)$$

$$\frac{\partial T}{\partial t} + U\frac{\partial T}{\partial X} + V\frac{\partial T}{\partial Y} = \frac{1}{Pr}\frac{\partial^2 T}{\partial Y^2} \quad (7)$$

with the following initial and boundary conditions:

$$\left.\begin{array}{lll} t \le 0,\ U = 0,\ V = 0,\ T = 0 & & \\ t > 0,\ U = 0,\ V = 0,\ T = x^n & \text{at } Y = 0 & \\ U = 0,\ T = 0 & \text{at } X = 0 & \\ U \to 0,\ T \to 0 & \text{as } Y \to \infty\ . & \end{array}\right\} \quad (8)$$

where

$$X = x/L,\ Y = \frac{y}{L}\,Gr_L^{1/4},\ U = \frac{uL}{\nu}\,Gr_L^{-1/2}$$

$$V = \frac{vL}{\nu}\,Gr_L^{-1/4},\ t = \frac{\nu t'}{L^2}\,Gr_L^{1/2},\ T = \frac{T' - T'_\infty}{T'_w - T'_\infty}$$

$$Gr_L = \frac{g\beta L^3 (T'_w - T'_\infty)}{\nu^2},\ Pr = \frac{\nu}{\alpha} \quad (9)$$

are non-dimensional quantities.

Here L is the length of the plate, Gr_L the Grashof number and Pr is the Prandtl number. Also, T'_w is the plate temperature.

These non-linear partial differential equations, subject to the initial and boundary conditions, are solved by using implicit finite-difference equations of Crank-Nicolson type which are discussed by Soundalgekar and Ganesan[5]. The equivalent finite-difference equations (5) to (8) are as follows:

$$\frac{U_{ij}^{n+1} - U_{i-1,j}^{n+1} + U_{ij}^{n} - U_{i-1,j}^{n} - U_{ij-1}^{n+1} - U_{i-1,j-1}^{n+1} + U_{ij-1}^{n} - U_{i-1,j-1}^{n}}{4\Delta X} + \frac{V_{ij}^{n+1} - V_{i,j-1}^{n+1} + V_{ij}^{n} - V_{i,j-1}^{n}}{2\Delta Y} = 0$$

$$\frac{U_{ij}^{n+1} - U_{ij}^{n}}{\Delta t} + U_{ij}^{n}\left[\frac{U_{ij}^{n+1} - U_{i-1,j}^{n+1} + U_{ij}^{n} - U_{i-1,j}^{n}}{2\Delta X}\right] +$$

$$V_{ij}^{n}\left[\frac{U_{i,j+1}^{n+1} - U_{i,j-1}^{n+1} + U_{i,j+1}^{n} - U_{ij-1}^{n}}{4\Delta Y}\right] = T_{ij}^{n+1} +$$

$$V_{ij}^{n}\left[\frac{U_{ij+1}^{n+1} - U_{ij-1}^{n+1} + U_{ij+1}^{n} - U_{ij-1}^{n}}{4\Delta Y}\right] = T_{ij}^{n+1} + \tag{11}$$

$$\frac{U_{ij-1}^{n+1} - 2U_{ij}^{n+1} + U_{ij+1}^{n+1} + U_{ij-1}^{n} - 2U_{ij}^{n} + U_{ij-1}^{n}}{2(\Delta Y)^2}$$

$$\left[\frac{T_{ij}^{n+1} - T_{ij}^{n} + U_{ij}^{n}}{\Delta t}\right]\left[\frac{T_{ij}^{n+1} - T_{i-1,j}^{n+1} + T_{ij}^{n} - T_{i-1,j}^{n}}{2\Delta X}\right]$$

$$+ V_{ij}^{n+1}\left[\frac{T_{ij+1}^{n+1} - T_{ij-1}^{n+1} + T_{ij+1}^{n} - T_{ij-1}^{n}}{4\Delta Y}\right] = \tag{12}$$

$$\frac{1}{Pr}\left[\frac{T_{1,j-1}^{n+1} - 2T_{ij}^{n+1} + T_{i,j+1}^{n+1} + T_{i,j-1}^{n} - 2T_{ij}^{n} + T_{i,j+1}^{n}}{2(\Delta Y)^2}\right].$$

Numerical technique

To solve the above set of equations, we consider a rectangular region such that the height of the plate is assumed to be $X_{max} = 1$ and the other side is given by $Y_{max}(= 14)$ where Y_{max} corresponds to $Y = \infty$, which lies well outside both the momentum and energy boundary layers. The maximum value of Y is chosen as 14 after some preliminary investigations so that the last two boundary conditions (8) are satisfied (i.e. $U \to 0$, $T \to 0$ as $Y \to \infty$). Here, i designates the X-direction, j the Y-direction and n the t-direction. Since the boundary layer thickness increases rapidly along the flow direction, i.e. X-direction, near the leading edge, the small mesh size is considered near the entrance region as follows:

$\Delta X = 0.01, \quad 0 < x < 0.2$
$= 0.05, \quad 0.2 < x < 1$

where $\Delta X = X_i - X_{i-1}$ and along the Y-direction, $\Delta Y = 0.25$, where $\Delta Y = Y_i - Y_{i-1}$ with time step $\Delta t = 0.01$.

After experimenting with a few sets of mesh sizes, the above-mentioned mesh sizes and time step have been fixed. In this case, spatial mesh sizes are reduced by 50 per cent in one direction, and later in both directions, and results are compared. It is observed that, when the mesh size is reduced by 50 per cent in the Y-direction (total number of grid-points are 37×113), the results differ in the fifth decimal place, while the mesh sizes are reduced by 50 per cent in X-direction (total number of grid-points are 73×57) or in both directions (total number of grid-points are 73×113) the results differ in the fourth decimal places. In all the above cases the time step level is reduced by 50 per cent and results are compared, there is no significant difference in the results up to the fifth decimal place. Hence, the above mentioned mesh sizes and time step have been considered as appropriate values for ΔX, ΔY, and Δt for calculation.

The total number of grid-points in the rectangular region which have been considered as a region of integration are 37×57.

At a particular time level n, finite difference equation (12) at every internal nodal point on a particular i-level constitutes a tridiagonal system of equations. The system of equation is solved by the Thomas algorithm as described in Carnahan *et al.*[9]. Thus the values of T are known at every nodal point on a particular i at $(n + 1)$th time level. Similarly, the values of U are calculated from equation (11) and, finally, the values of V are calculated explicitly using equation (10) at every nodal point on a particular i-level at $(n + 1)$th time level. In a similar manner, computations are carried out by moving along the i-direction. After computing values corresponding to each i at $(n + 1)$th time level, the values at the next time level are determined in a similar fashion. Computations are carried out until the steady-state is reached. The steady-state solution is assumed to have been reached when the absolute differences between values of velocity as well as temperature T at two consecutive time steps are less than 10^{-5} at all grid-points.

Results and discussions

In order to check the accuracy of our computed values, we compare our results for steady-state values of U and T with those of the curves computed by Gebhart and Pera[10] and Sparrow and Gregg[7] for values of $X = 0.1$, 0.5, 1.0 and for air. These are plotted in Figure 1. We observe that for both $n = 0$ and 3.0, there is a good agreement. In Figure 2, temperature profiles are shown for air ($Pr = 0.7$) and $n = 0$. Our results agree very well with those of Gebhart and Pera's[10] results for all values of X, i.e. near the leading edge as well as at $X = 1.0$, a slight distance from the leading edge. In Figure 3, the temporal maximum and the steady-state values of velocity for different values of Pr, n and X are plotted. We observe from this figure that an increase in Pr or n leads to a

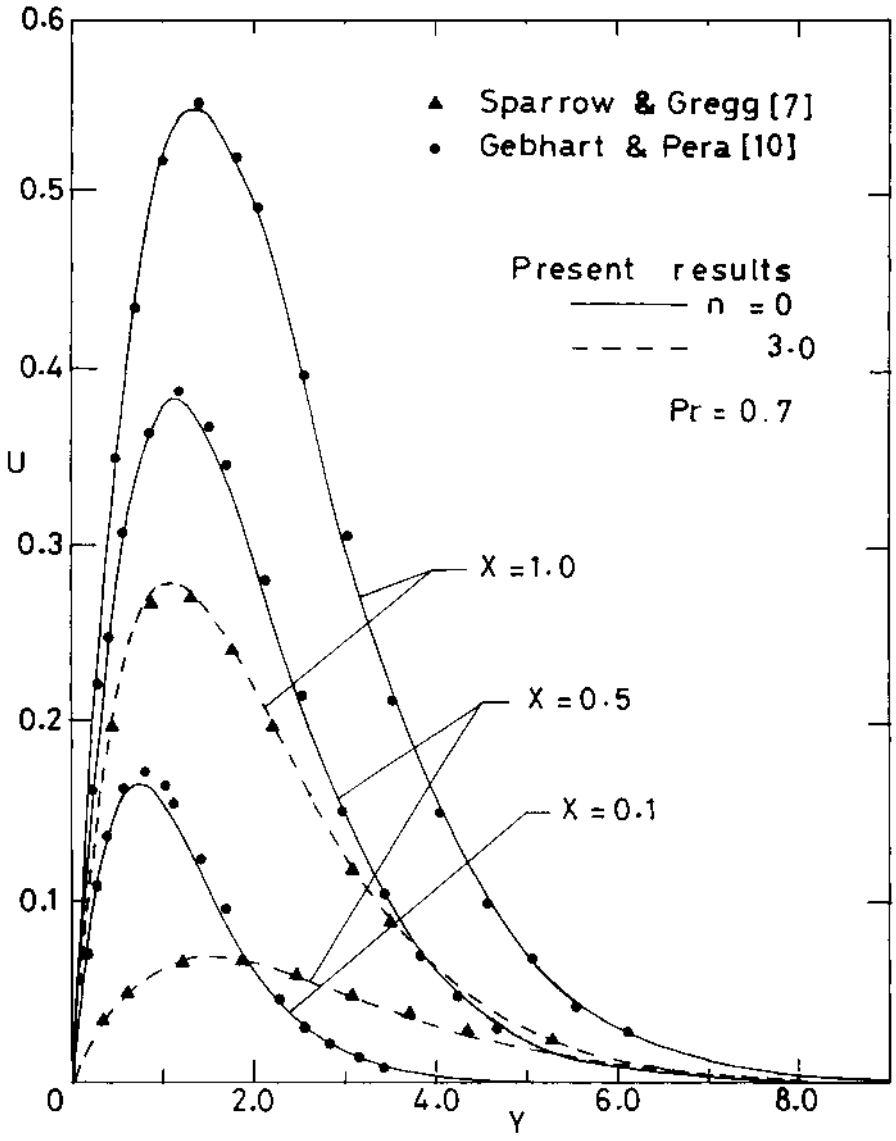

Figure 1. Comparison of steady-state velocity profiles at different values of X

decrease in the value of the temporal maximum of velocity and also in the value of steady-state velocity. For uniform plate temperature, we observe a remarkable difference between the temporal maximum value and the steady-state maximum value. Conversely, for non-uniform plate temperature, this difference starts diminishing as n increases. However, at large values of Pr, such a difference does not exist at all.

In Figure 4, the transient and steady-state temperature profiles are shown for both X = 1.0 and 0.1. We observe from this figure that, owing to non-uniformity

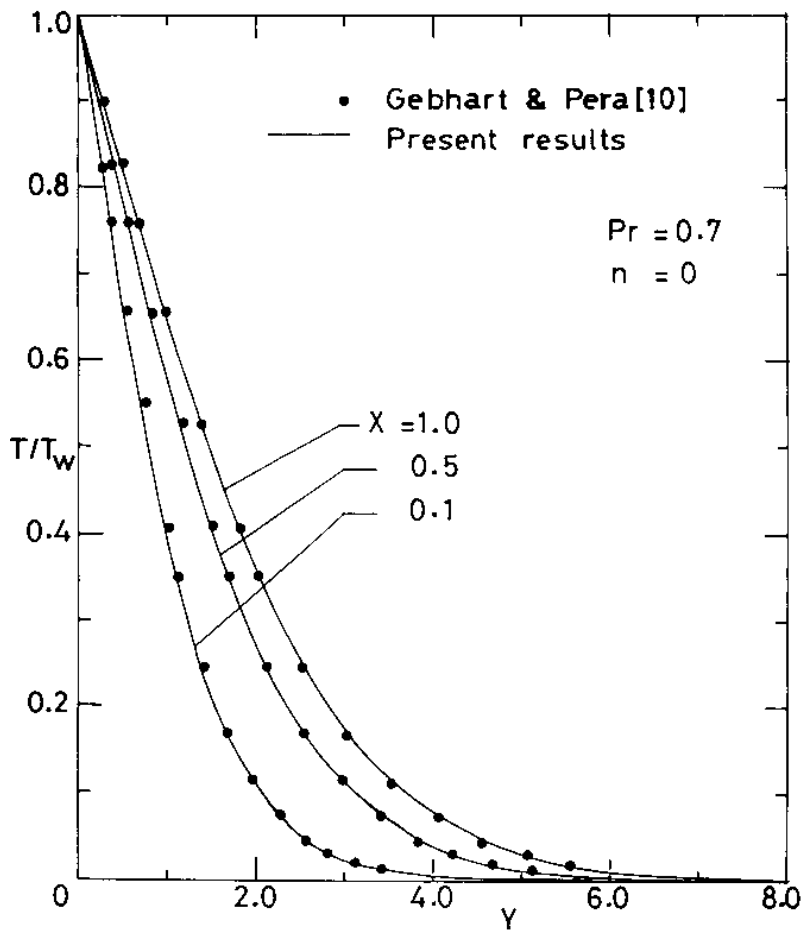

Figure 2.
Comparison of steady-state temperature profiles at different values of X

of plate temperature, there is a fall in the transient as well as steady-state temperature of the fluid and, as n increases, the time required to reach steady-state is greater, for near the edge of the plate, as compared to that at a large distance from the leading edge.

In Figure 5, the steady-state velocity profiles for air are shown for different values of n and X. We observe from this figure that the steady-state velocity decreases as n increases at all the positions from the leading edge. Hence, the proximity of the leading edge has no effect on the steady-state, but non-uniformity of plate temperature has a prominent effect.

In Figure 6, the effect of distance of the leading edge on the steady-state temperature is shown for air. We observe from this figure that far away from the leading edge, say at $X = 1.0$, the temperature is found to be falling as n increases, except at $n = 1$. However, at $n = 1$, the plate temperature increases uniformly with distance from the leading edge and the steady-state temperature remains the same.

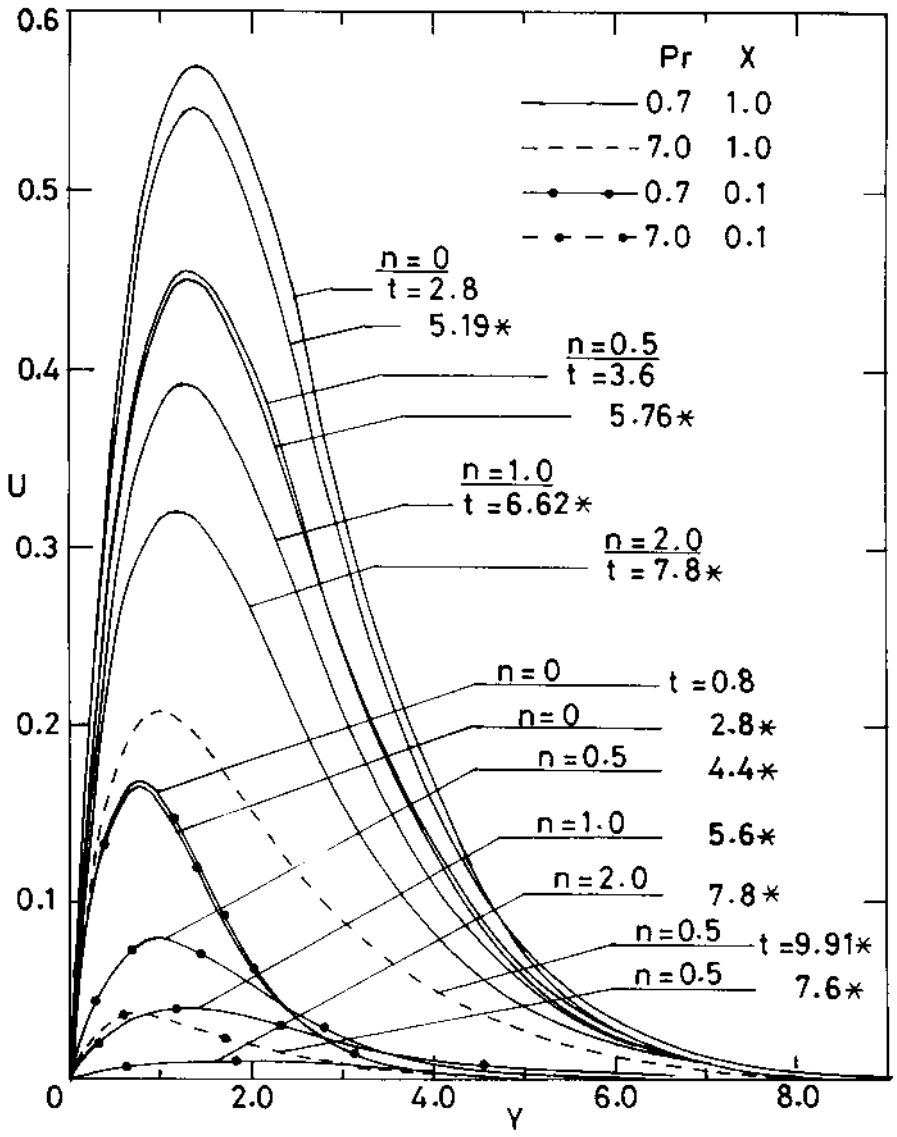

Figure 3.
Transient velocity profiles for different values of *Pr*, *n* and *X* (* is the steady-state value)

Local skin-friction and heat transfer

From the velocity and temperature fields, we now study the local and average skin friction and the Nusselt number. These are given by:

$$\tau_x = \mu \left(\frac{\partial u}{\partial y} \right)_{y=o} \tag{13}$$

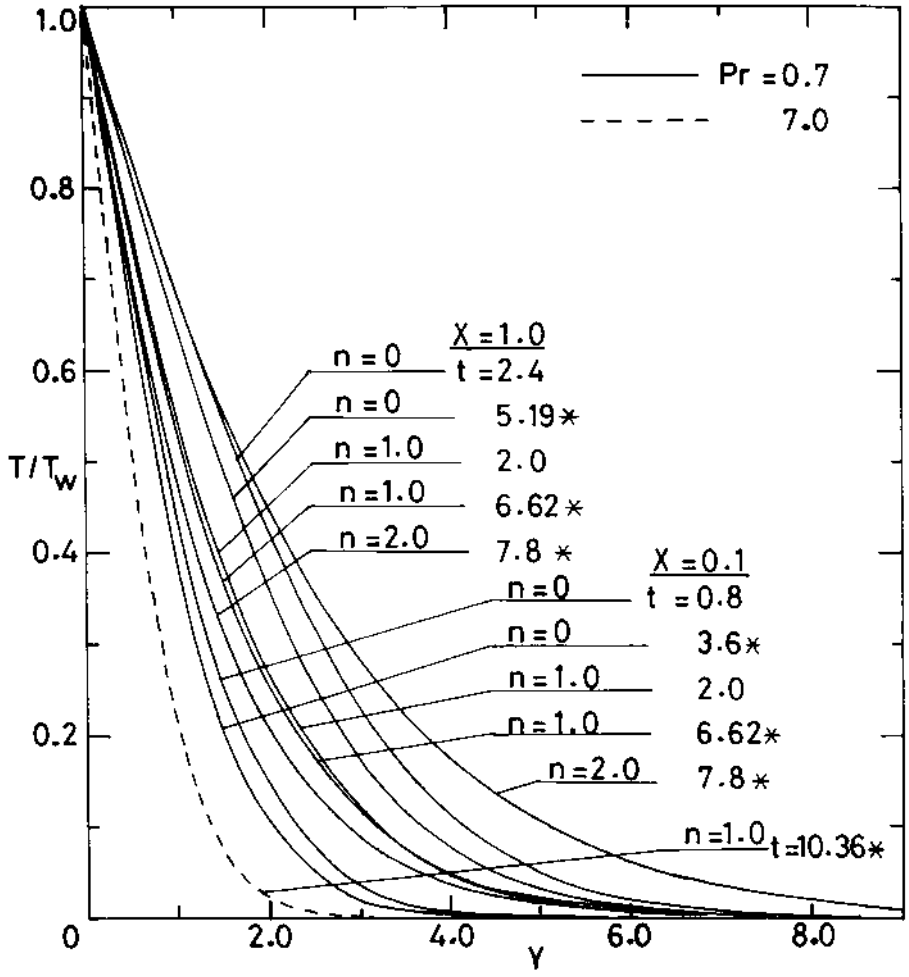

Figure 4.
Transient temperature profiles for different values of *Pr*, *N* and *X*. (* is the steady state value)

$$\bar{\tau}_L = \frac{1}{L}\int_0^L \mu \left(\frac{\partial u}{\partial y}\right)_{y=o} dx \tag{14}$$

$$Nu_x = -x\left(\frac{\partial T'}{\partial y}\right)_{y=o} /(T'_w - T'_\infty) \tag{15}$$

$$\bar{Nu}_L = -\int_0^L \left[\left(\frac{\partial T'}{\partial y}\right)_{y=o} /(T'_w - T'_\infty)\right] dx \tag{16}$$

and in view of relations (9), equations (13) to (15) reduce to the following non-dimensional forms:

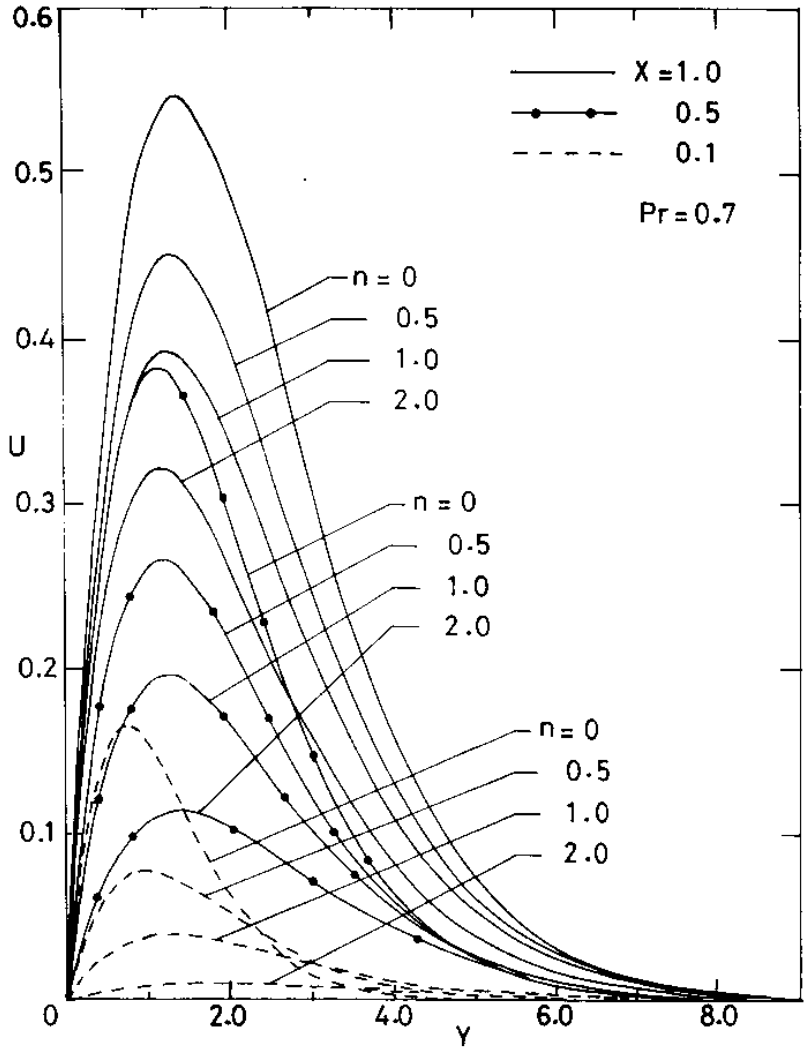

Figure 5.
Steady state velocity profiles for different values of n and X

$$\tau_x = Gr_L^{3/4} \left[\frac{\partial U}{\partial Y} \right]_{Y=0} \tag{17}$$

$$\bar{\tau}_L = Gr_L^{3/4} \int_0^1 \left[\frac{\partial U}{\partial Y} \right]_{Y=0} dX \tag{18}$$

and

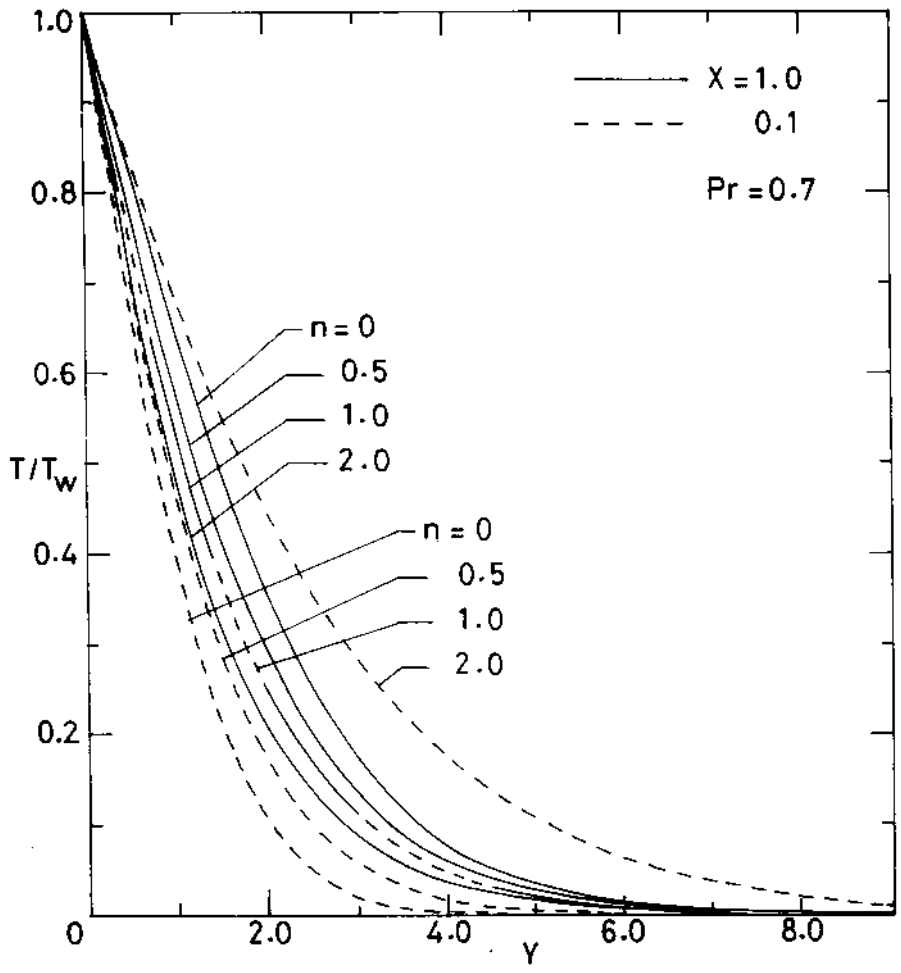

Figure 6.
Steady state temperature profiles for different values of n and X

$$Nu_x = \frac{-X\left(\frac{\partial T}{\partial Y}\right)_{Y=o} Gr_L^{1/4}}{T_{Y=o}} \tag{19}$$

$$\overline{Nu} = -Gr_L^{1/4}\int_o^1 \left[\left(\frac{\partial T}{\partial Y}\right)_{Y=o} / T_{Y=o}\right] dX \tag{20}$$

The values of τ_X are evaluated by a five-point approximate formula for the derivative and then the integral for $\overline{\tau}$ is evaluated by the use of the Newton-Cotes closed integration formula. These are shown in Figures 7 to 11.

We observe from Figure 7 that the local skin-friction decreases with increasing the Prandtl number Pr or n. From Figure 8, we observe that the local Nusselt number increases with increasing the Prandtl number, but decreases with increasing n near the leading edge and increases with increasing n at a distance away from the leading edge. From Figure 9, it can be seen that the average skin-friction decreases with increasing the Prandtl number Pr, but decreases with increasing n. However, at small values of time, $t < 2.5$, the average number is found to increase with time and, after $t > 2.5$, its values remain almost unaffected by time, i.e. the skin-friction reaches the stationary state after $t \approx 2.5$. From Figure 10, the average Nusselt number is seen to fall sharply at small values of time, t, and then it remains unaffected by time. It is interesting to note here that it reaches its maximum value when n increases from 0 to 0.66 and then onward, it decreases with increasing n.

In order to compare our numerical results for Nusselt number evaluated by finite-difference technique, we have plotted our results for $Pr = 1.0$ and 0.7 and also those derived by Sparrow and Gregg[7] on Figure 11 and our results are found to agree well with those of Sparrow and Gregg for values of $n > 0$.

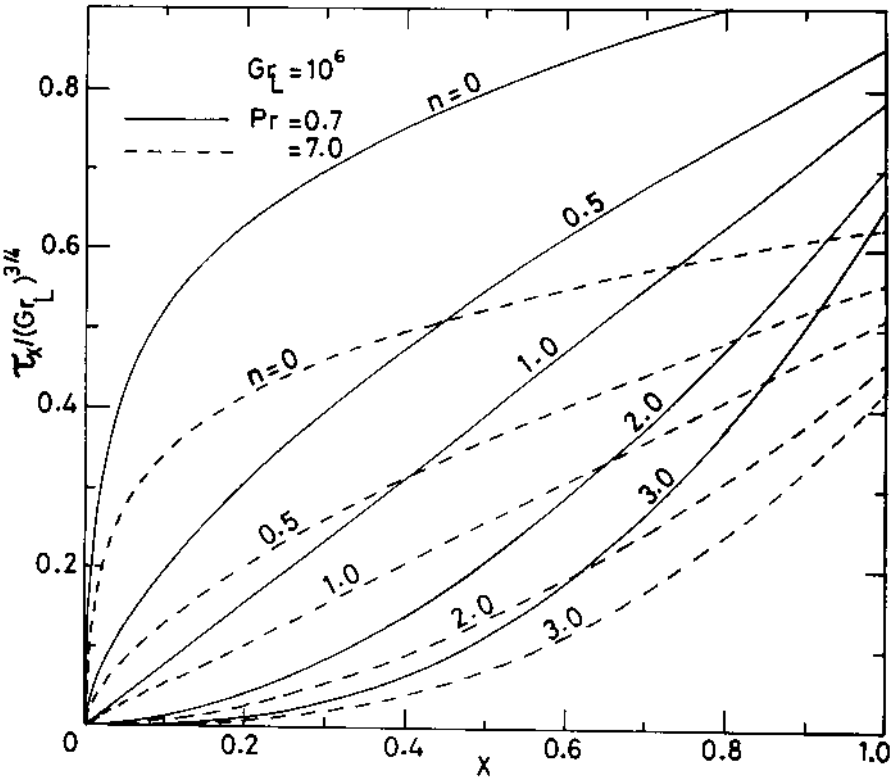

Figure 7.
Local skin-friction

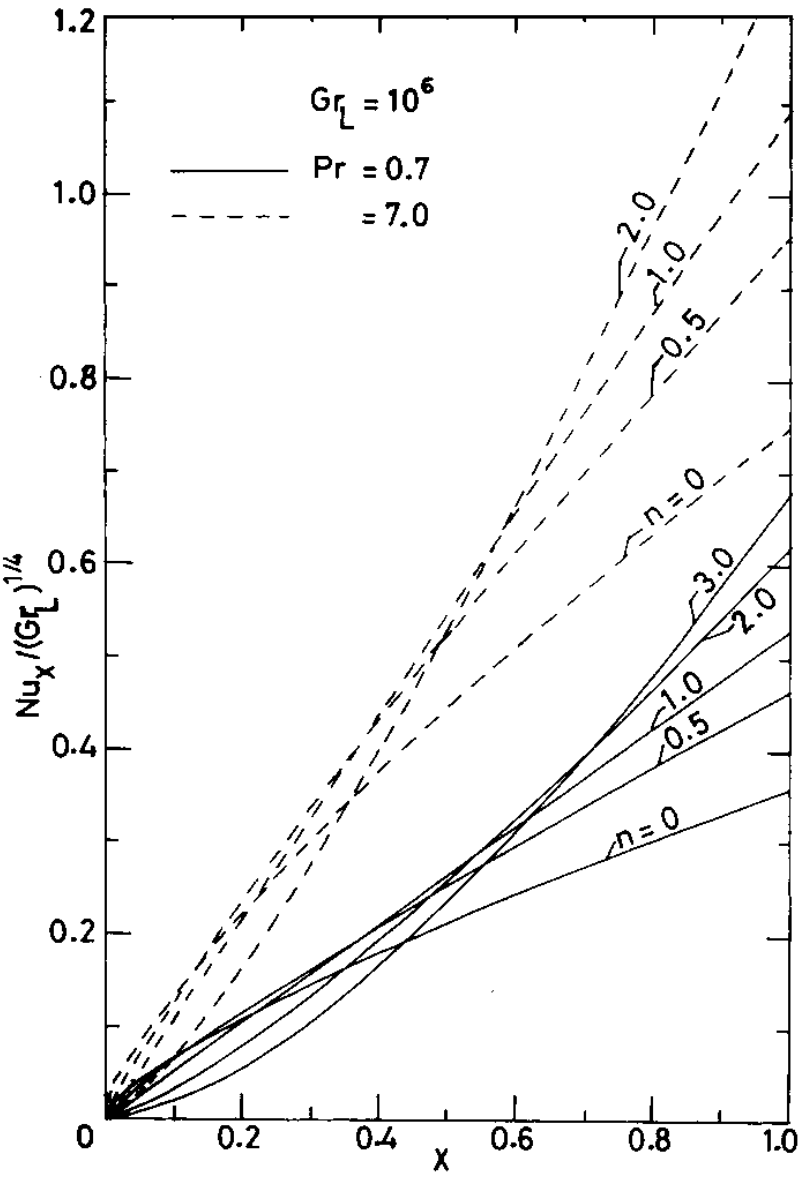

Figure 8.
Local Nusselt number

From the numerical results for the isothermal plate, the local Nusselt number, Nu_x in the steady-state, can be expressed as a function of Gr_L, and Pr as

$$Nu_x = 0.394\ (Gr_L\ Pr)^{1/4} \tag{21}$$

and this is in good agreement with the experimental results of Al-Arabi and Sakr[11]. For variable temperature on the plate, Chen *et al.* [12] expressed this correlation coefficient as a function of the Prandtl number Pr. It is found that the

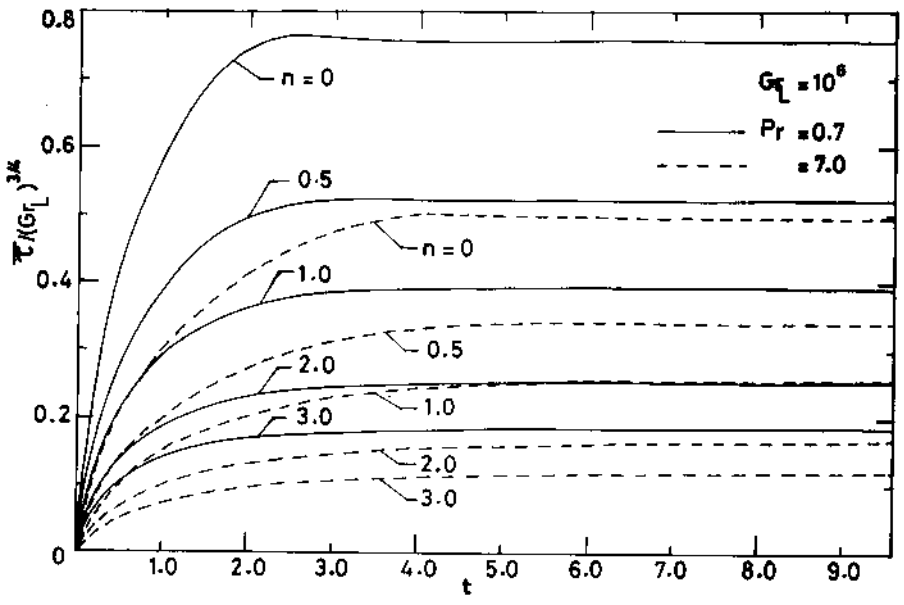

Figure 9.
Average skin-friction

present numerical results correlate well with those results of Chen *et al.* within a maximum error of 3 per cent. In the present study, we observe that the constant of proportionality depends on the exponent n and can be shown to be given as:

$$\mathrm{Nu}_x = \mathrm{K(Pr,n)}\ (\mathrm{Gr}_L \mathrm{Pr})^{1/4} \tag{22}$$

where

$$K(Pr,n) = \frac{3}{4}\left[\frac{2Pr(1+4n)}{5(1+2Pr^{1/2}+2Pr)}\right]^{1/4}.$$

Again in the present study the numerical results of the average Nusselt number are in agreement with the correlation equation for uniform wall temperature given by Chen *et al.*[12] with a maximum error of 13 per cent. It is also observed that the constant of proportionality depends on Pr and n and a new correlation coefficient $K1(Pr,n)$ is arrived at. The same is shown here

$$Nu = K1(\mathrm{Pr},n)\,(Gr_L\ \mathrm{Pr})^{1/4} \tag{23}$$

where

$$K1(Pr,n) = \left[\frac{Pr(1+0.223n^{1/4})}{3(1+Pr^{1/2}+Pr)}\right]^{1/4}.$$

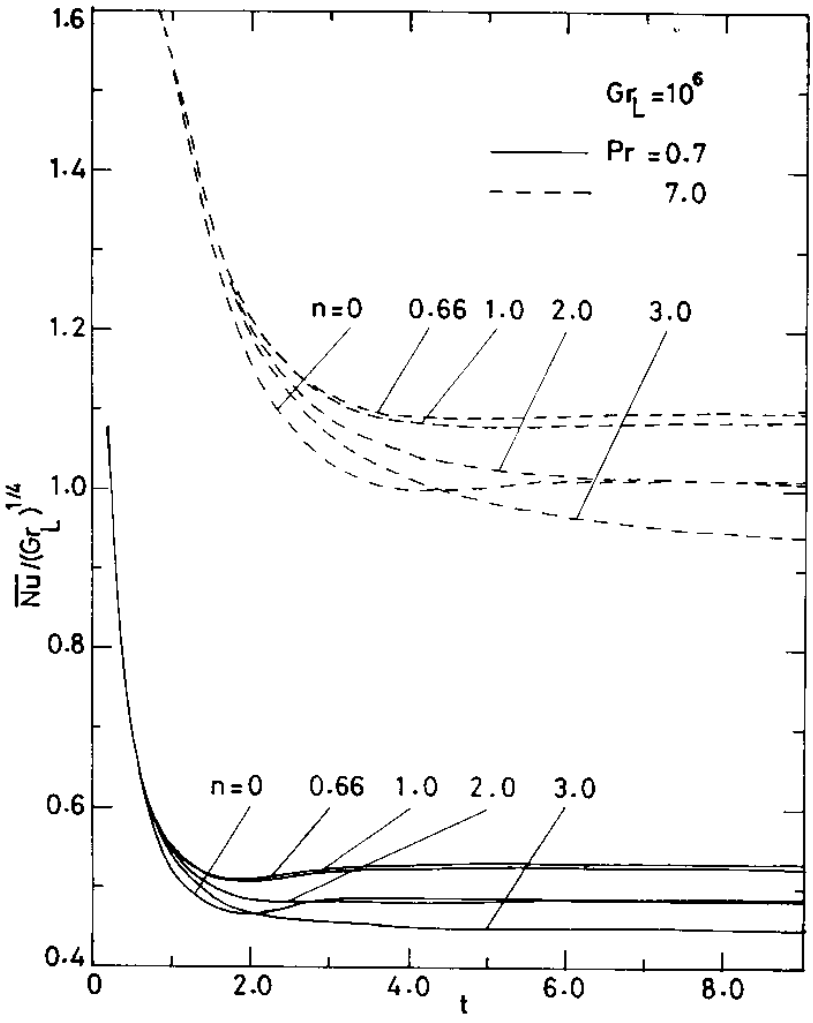

Figure 10.
Average Nusselt number

The numerical results are in good agreement with the above correlation with a maximum error of 6 per cent.

Conclusions

In this paper, transient natural convection in laminar boundary layer flows over a non-isothermal vertical plate has been studied numerically for the case of power-law variation of wall temperature. We summarize here the major findings.

- For air (Pr = 0.7), it takes longer to reach the steady-state as the exponent n increases.

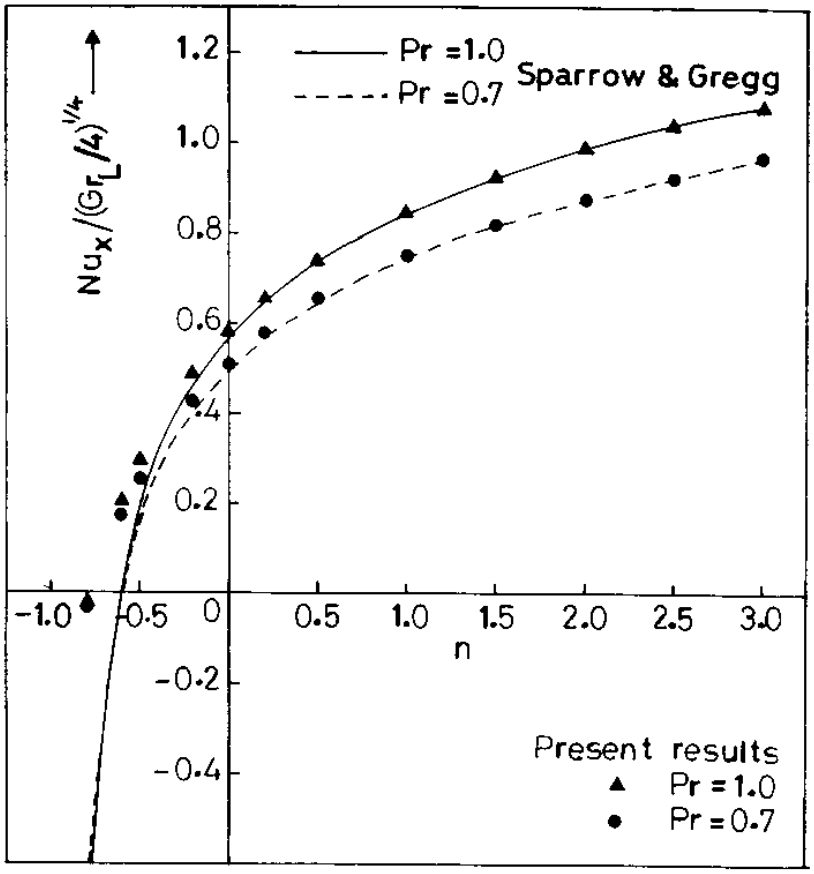

Figure 11.
Comparison of local Nusselt number

- Time to reach the steady-state increases with increasing Prandtl number.
- The difference between the temporal maximum value and the steady-state value of both velocity and temperature decreases as n or Pr increases.
- The steady-state local skin-friction falls with increasing exponent n and the Prandtl number.
- The average skin-friction increases steeply in the initial stages and it decreases with n.
- The steady-state local Nusselt number increases with increasing exponent n for large values of x and at small values of x, it decreases with increasing n. It also increases with increasing Pr.
- The average Nusselt number reaches its maximum value when $n = 0.66$ and then onward, it decreases with increasing n.

References

1. Pohlhausen, E., "Der Wärmeaustausch zwischen festen körpern und Flüssingkeiten mit kleiner Reibung und kleiner Wärmeleitung", *Z. Angew. Math. Mech.*, Vol. 1, 1921, pp. 115-21.
2. Ostrach, S., "An analysis of laminar free convection flow and heat transfer about a flat plate parallel to the direction of the generating body force", *NACA Report*, No. 1111, 1953, pp. 63-79.
3. Seigel, R., "Transient free convection from a vertical flat plate", *Transactions of the American Societies of Mechanical Engineers*, Vol. 80, 1958, pp. 347-59.
4. Hellums, J.D. and Churchill, S.W., "Transient and steady state free and natural convection, numerical solution: part 1, the isothermal vertical plate", *American Institute of Chemical Engineers Journal*, Vol. 8, 1962, pp. 690-2.
5. Soundalgekar, V.M. and Ganesan, P., "Finite difference analysis of transient free convection on an isothermal flat plate", *Reg. J. Energy Heat Mass Transfer*, Vol. 3, 1981, pp. 219-24.
6. Ede, A.J., "Advances in free convection", in Irvine, T.F. and Hartnett, J.P. (Eds), *Advances in Heat Transfer*, Vol. 4, Academic Press, 1968, pp. 1-64.
7. Sparrow, E.M. and Gregg, J.L., "Similar solutions for free convection from a non-isothermal vertical plate", *Transactions of ASME, Journal of Heat Transfer*, Vol. 80, 1958, pp. 379-86.
8. Raithby, G.D. and Hollands, K.G.T., "Natural convection", in Rohsenow, W.M., Hartnett, J.D. and Ganic, E.N. (Eds), *Handbook of Heat Transfer Fundamentals*, McGraw-Hill, New York, NY, 1985.
9. Carnahan, B., Luther, H.A. and Wilkes, J.O., *Applied Numerical Methods*, John Wiley & Sons, New York, NY, 1969.
10. Gebhart, B. and Pera, L., "The nature of vertical natural convection flows resulting from the combined buoyancy effects of thermal and mass diffusion", *International Journal of Heat Mass Transfer*, Vol. 14, 1971, pp. 2025-50.
11. Al-Arabi, M. and Sakr, B., "Natural convection heat transfer from inclined isothermal plates", *International Journal of Heat Mass Transfer*, Vol. 31, 1988, pp. 559-66.
12. Chen, T.S., Tien, H.C. and Armaly, B.F., "Natural convection on horizontal, inclined, and vertical plates with variable surface temperature or heat flux", *International Journal of Heat Mass Transfer*, Vol. 29, 1986, pp. 1465-78.